



Narrow-band deep-ultraviolet light emitting device using Al_{1-x}GdxN

Kita, Takashi ; Kitayama, Shinya ; Kawamura, Masashi ; Wada, Osamu ; Chigi, Yoshitaka ; Kasai, Yoshihiro ; Nishimoto, Tetsuro ; Tanaka,...

(Citation)

Applied Physics Letters, 93(21):211901-211901

(Issue Date)

2008-11-24

(Resource Type)

journal article

(Version)

Version of Record

(URL)

<https://hdl.handle.net/20.500.14094/90000743>



Narrow-band deep-ultraviolet light emitting device using $\text{Al}_{1-x}\text{Gd}_x\text{N}$

Takashi Kita,^{1,a)} Shinya Kitayama,¹ Masashi Kawamura,¹ Osamu Wada,¹ Yoshitaka Chigi,² Yoshihiro Kasai,¹ Tetsuro Nishimoto,² Hiroyuki Tanaka,² and Mikihiro Kobayashi²

¹Department of Electrical and Electronics Engineering, Graduate School of Engineering, Kobe University, Rokkodai 1-1, Nada, Kobe 657-8501, Japan

²YUMEX INC., Itoda 400, Yumesaki, Himeji, Hyogo, 671-2114, Japan

(Received 30 September 2008; accepted 28 October 2008; published online 24 November 2008)

We demonstrated mercury-free narrow-band deep-ultraviolet luminescence from field-emission devices with $\text{Al}_{1-x}\text{Gd}_x\text{N}$ thin films. The $\text{Al}_{1-x}\text{Gd}_x\text{N}$ thin films were grown on fused silica substrates by a radio frequency reactive magnetron sputtering method. The deposited film shows a strong *c*-axis preferential orientation. A resolution limited, narrow intra-4*f* luminescence line from Gd^{3+} ions has been observed at 315 nm. The luminescence spectrum depends on the growth temperature of the thin film, and the intensity varies as a function of the GdN mole fraction. © 2008 American Institute of Physics. [DOI: 10.1063/1.3028341]

After invention of mercury lamp in 1927, the ultraviolet (UV) light emitted from the lamp has been widely used in various industrial processes such as photopolymerization and photolithography for large display panels and printed circuit boards. The light emission in the UV region, moreover, is known to be suitable for sterilization and medical treatments for incurable skin diseases. However, mercury is a serious toxic element. For human life free from mercury, development of novel UV lighting devices is indispensable. Recently, nitride-semiconductor based light emitting diodes (LEDs) have been attracting strong interest in the UV region.¹ LEDs emitting at 365 nm matching with the *i* line of the mercury lamp are already in the market, and the emission power of 250 mW has been achieved for the commercial devices.² On the other hand, an ultimate short wavelength emission at 210 nm has been demonstrated by using a AlN homojunction, though the output power is still very weak.³ The use of quantum well structures in the LEDs is suitable for accomplishing the desired wavelength and efficient light emission. However, the spectral line width limited by the thermal carrier distribution in the quantum structure is broad over ~10 nm. Much narrower spectral width is necessary for many applications such as the photolithography and medical applications.

On the other hand, rare earth ions are easy to create narrow band luminescence because of the intraorbital electron transitions, which are usually used in conventional fluorescent lights, cathode-ray tubes, plasma-display panels, and so on. The intraorbital electron transition is generally dipole forbidden, and, therefore, the radiative decay lifetime is long. Furthermore, the spectrum is insensitive to the environment because of the electromagnetic shield effect caused by the occupied outer shells. In particular, Gd^{3+} ion efficiently emits UV luminescence at about 310 nm. That is the transition from ${}^6P_{7/2}$ of the excited states to the ground state ${}^6S_{7/2}$ in the 4*f* orbital. Such intra-4*f* electron transition shows an extremely narrow band emission line. To obtain lossless, efficient UV emission from Gd^{3+} ions, a host material with the energy band gap more than about 4 eV is necessary. Several works have reported that AlN is a good host material for

Gd^{3+} ions^{4–7} because of the large band gap of about 6 eV and the isoelectronic properties of the Gd^{3+} centers replacing Al^{3+} ions. Moreover, AlN is known to be a thermally and chemically stable material.

In this study, we developed field-emission devices (FEDs) with $\text{Al}_{1-x}\text{Gd}_x\text{N}$ thin films. The accelerated electrons excite the $\text{Al}_{1-x}\text{Gd}_x\text{N}$ thin film, and the narrow band luminescence line is obtained at 315 nm. The $\text{Al}_{1-x}\text{Gd}_x\text{N}$ thin films were grown on fused silica substrates by a radio frequency (rf) reactive magnetron sputtering method. The luminescence characteristics depending on the GdN mole fraction and the growth temperature are discussed.

We grew $\text{Al}_{1-x}\text{Gd}_x\text{N}$ thin films on fused silica substrates at 500 °C by a rf reactive magnetron sputtering technique.⁸ The deposition chamber whose back pressure is about 6×10^{-6} Pa is separated from a chamber for introducing the substrate. We used ultrapure (6*N*) mixed gas of argon and nitrogen for the reactive growth. The total pressure was 5 Pa, and the partial pressure ratio was even. Metal targets used here are Al (4*N*) and Gd (3*N*). When we grow $\text{Al}_{1-x}\text{Gd}_x\text{N}$, we set Gd metal tips on the Al target. The doping concentration was controlled by changing the number of the tips. The input rf power was 250 W.

Figure 1(a) shows a typical x-ray diffraction spectrum of an AlN film. The film thickness is 400 nm. The spectrum shows a strong *c*-axis preferential orientation. The in-plane orientation examined by the x-ray pole figure measurement was random. Therefore, the deposited film is the *c*-axis oriented polycrystal. The full width at the half maximum of the (0002) x-ray rocking curve is less than 6°. The optical band gap of the AlN film was examined by the optical reflectance shown in Fig. 1(b). The derivative reflectance spectrum shows a distinct interference structure vanishing at ~200 nm, which indicates that the band-gap energy is almost same as that of a high-quality bulk crystal.⁹ In this work, we have grown $\text{Al}_{1-x}\text{Gd}_x\text{N}$ thin films with different Gd concentrations. The x-ray diffraction spectra of these doped films are shown in Fig. 2. The film thickness of these films is 1080 nm. The Gd concentration was measured by using the electron probe micro analyzer. When the GdN mole fraction is over about 10%, the spectrum changes dramatically. The diffraction intensity remarkably decreases, and some diffrac-

^{a)}Electronic mail: kita@eedept.kobe-u.ac.jp.

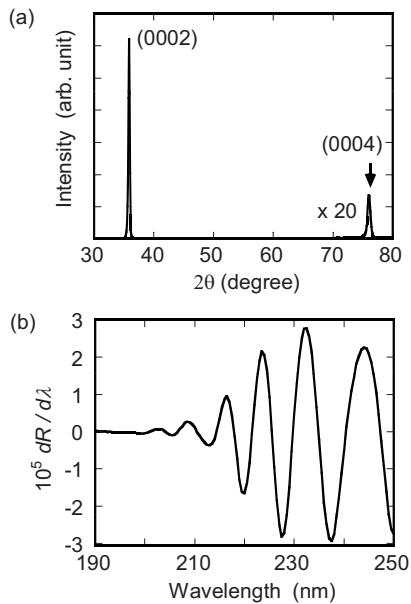


FIG. 1. X-ray diffraction spectrum (a) and first-derivative reflectance spectrum (b) of an AlN film.

tion signals originated from the Gd-metal phase appear instead. The crystal symmetry of the bulk AlN is wurtzite, and the a -axis and c -axis lattice constants are $a_{\text{AlN}}=0.3112$ nm and $c_{\text{AlN}}=0.4982$ nm, respectively.¹⁰ Since the bulk GdN has the rocksalt structure with the larger c -axis lattice space of $a_{\text{GdN}}[222]=0.5772$ nm,¹¹ the crystal structure of AlN containing a great many Gd atoms becomes unstable. Therefore, the excess Gd atoms are considered to be separated from the $\text{Al}_{1-x}\text{Gd}_x\text{N}$ phase.

There are several reports about luminescence from Gd-doped AlN, where fundamental luminescence properties of doped Gd^{3+} ions have been discussed.^{4–6} Here, in order to develop an electrically driven mercury-free narrow-band deep-UV lighting device, we fabricated FEDs with the $\text{Al}_{1-x}\text{Gd}_x\text{N}$ films. The FED structure used is illustrated in Fig. 3(a). The electron emitter was set at a side electron emission configuration,¹² which is suitable for extracting the emitted light efficiently. The device consists of a cathode electrode, carbon nanofiber/elastomer nanocomposite sheets as the electron emitter, a thin insulating spacer sheet with 300 μm thickness, and an invar alloy grid-type anode electrode.¹² We used a phosphor bronze alloy for the cathode electrode. The grid-type electrode was contacted with the $\text{Al}_{1-x}\text{Gd}_x\text{N}$ film, where the window area of the grid is $10 \times 8 \text{ mm}^2$. Field-emitted electrons were extracted by applying a negative bias to the emitter against the grid electrode, which irradiate the $\text{Al}_{1-x}\text{Gd}_x\text{N}$ film as drawn by white arrows. All FED measurements were carried out at room temperature in a vacuum of 6.5×10^{-4} Pa. A typical electron emission profile is shown in Fig. 3(b). Bright electron emission current over 1 μA was obtained in the saturation region appeared above the applied voltage of about 300 V. We used this region for the excitation.

Figure 4(a) shows a typical luminescence spectrum measured at 100 μA . The film thickness used in the FED is 135 nm. A sharp luminescence line is observed at 315 nm. A weak, broad signal around 500 nm is considered to be due to the oxygen-related defect luminescence¹³ and/or the fused silica substrate.¹⁴ The UV narrowband emission appeared clearly when the accelerated electron energy is more than

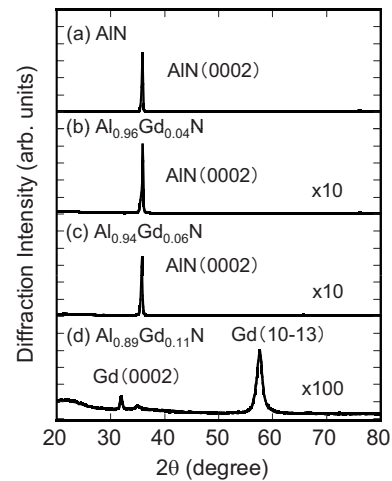


FIG. 2. X-ray diffraction spectra of AlN and $\text{Al}_{1-x}\text{Gd}_x\text{N}$ films with different GdN mole fractions.

1 keV. Because of the insulating feature of the AlGdN film on the fused silica substrate, it is considered that electrons losing their energy owing to negative charges on the film surface excite Gd^{3+} ions. The excitation and energy relaxation process is considered to be the same as the conventional cathodoluminescence^{4,5} and photoluminescence.⁶ The emission intensity has been found to show a linear dependence on the injection current in our current region up to 100 μA . We compare the Gd concentration dependence of the luminescence intensity measured at the same injection current of 100 μA . The results are summarized in the inset

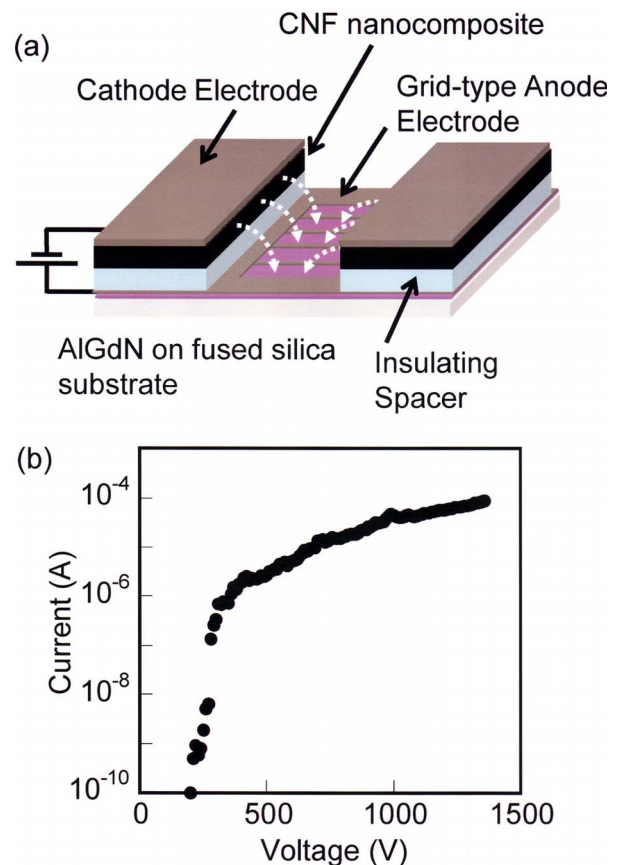


FIG. 3. (Color online) FED structure (a) and a typical electron emission characteristic measured as a function of the applied voltage between the cathode electrode and the grid type electrode.

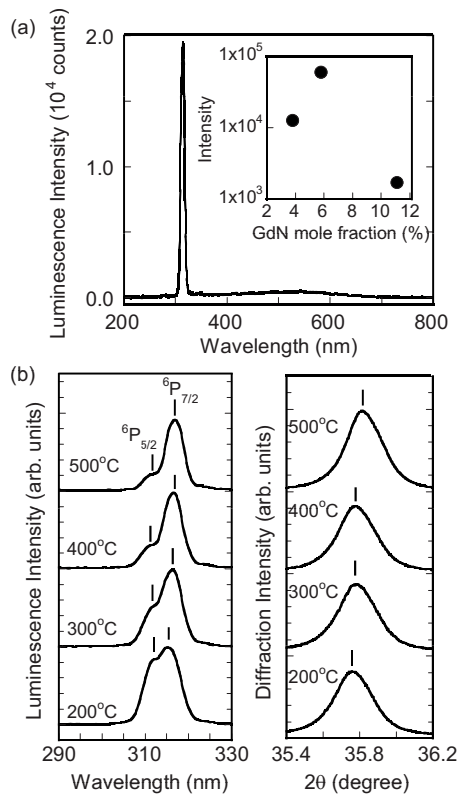


FIG. 4. A typical luminescence spectrum from the FED with an $\text{Al}_{0.94}\text{Gd}_{0.06}\text{N}$ film is shown in (a). The inset displays the GdN mole fraction dependence of the luminescence intensity at 315 nm. The left and right figures of (b) show the expanded luminescence spectra and the (0002) x-ray diffraction signals for $\text{Al}_{0.94}\text{Gd}_{0.06}\text{N}$ films grown at different temperatures, respectively.

of Fig. 4(a). The luminescence intensity increases with the GdN mole fraction. However, the film including the Gd metal phase shows the very weak luminescence because of the small amount of Gd^{3+} ions. The GdN mole fraction showing the strongest luminescence intensity was 6%.

The expanded luminescence spectrum is shown in Fig. 4(b). Here, we compare luminescence spectra for $\text{Al}_{0.94}\text{Gd}_{0.06}\text{N}$ films grown at different temperatures in the range of 200–500 °C. We controlled the current-voltage condition of the FED in order to operate at 100 μA . There was no clear difference in the current-voltage characteristics for the films grown at the different growth temperatures. Two signals are confirmed. The strong peak at 315 nm is attributed to the transition from the excited state ${}^6P_{7/2}$ to the ground state ${}^6S_{7/2}$. The spectral line width is about 4 nm, which corresponds to the resolution limit of our monochromator. We have confirmed a resolution limited spectrum even when using a higher-resolution monochromator with the spectral resolution of 1 nm. On the other hand, the weak signal appeared at the shorter wavelength side is due to the transition from ${}^6P_{5/2}$ to ${}^6S_{7/2}$. The signal intensity of the ${}^6P_{5/2}$ – ${}^6S_{7/2}$ transition depends on the splitting energy between the ${}^6P_{5/2}$ and ${}^6P_{7/2}$ states. In other words, population of excited electrons in the split excited states determines the spectral structure. We found that the relative intensity can be controlled by choosing the growth temperature of the $\text{Al}_{1-x}\text{Gd}_x\text{N}$ film. As shown in Fig. 4(b), with lowering the growth temperature, the splitting energy has been found to

decrease, and resultantly, the ${}^6P_{5/2}$ – ${}^6S_{7/2}$ transition intensity gradually increases. When the film was grown at 200 °C, both the intensities become almost the same. These changes in the splitting energy of the excited states is considered to be caused by the crystal field varied by the thermal expansion mismatch between the film and the substrate. Since the thermal expansion coefficient of AlN ($4.36 \times 10^{-6} \text{ K}^{-1}$) (Ref. 15) is about one order of magnitude larger than that of fused silica ($\sim 6 \times 10^{-7} \text{ K}^{-1}$),¹⁶ the higher temperature growth causes a stronger thermal expansion mismatch. Such biaxial tensile strain in $\text{Al}_{1-x}\text{Gd}_x\text{N}$ reduces the lattice space along the c axis, which leads to a slight peak shift of the (0002) x-ray diffraction signal as observed in Fig. 4(b). Therefore, the change in the splitting energy between the ${}^6P_{5/2}$ and ${}^6P_{7/2}$ states is caused by the different biaxial crystal fields.

In summary, electrically driven mercury-free narrow-band deep-UV luminescence has been demonstrated by using FEDs with $\text{Al}_{1-x}\text{Gd}_x\text{N}$ thin films. A resolution limited intra-4f luminescence line of Gd^{3+} ions was obtained by accelerated electrons emitted from the cathode electrode. The luminescence line corresponding to the transition from the excited state ${}^6P_{7/2}$ to the ground state ${}^6S_{7/2}$ appeared at 315 nm, and the spectral line width was found to be less than 1 nm. The luminescence spectrum depends on the growth temperature of the thin film, and the intensity varies as a function of the GdN mole fraction.

The authors would like to thank technical support about the FED and useful discussions with A. Magario and T. Noguchi of Nisshin Kogyo Co., Ltd. and H. Yanagi of Nara Institute of Science and Technology. This work was partly supported by Potentiality verification stage of Collaborative Development of Innovative Seeds, Japan Science and Technology Agency and Grant-in-Aid for Scientific Research on Priority Areas Grant No. 20048005.

¹M. A. Khan, M. Shatalov, H. P. Maruska, H. M. Wang, and E. Kuokstis, *Jpn. J. Appl. Phys., Part 1* **44**, 7191 (2005).

²http://www.nichia.co.jp/about_nichia/.

³Y. Taniyasu, M. Kasu, and T. Makimoto, *Nature (London)* **441**, 325 (2006).

⁴U. Vetter, J. Zenneck, and H. Hofsäss, *Appl. Phys. Lett.* **83**, 2145 (2003).

⁵J. B. Gruber, U. Vetter, H. Hofsäss, B. Zandi, and M. F. Reid, *Phys. Rev. B* **69**, 195202 (2004).

⁶J. M. Zavada, N. Nepal, J. Y. Lin, H. X. Jiang, E. Brown, U. Hömmerich, J. Hite, G. T. Thaler, C. R. Abernathy, and S. J. Pearton, *Appl. Phys. Lett.* **89**, 152107 (2006).

⁷M. Maqbool, I. Ahmad, H. H. Richardson, and M. E. Kordes, *Appl. Phys. Lett.* **91**, 193511 (2007).

⁸A. Kishimoto, Y. Inou, T. Kita, and O. Wada, *Phys. Status Solidi C* **4**, 2490 (2007).

⁹Q. Guo, M. Nishio, H. Ogawa, and A. Yoshida, *Phys. Rev. B* **64**, 113105 (2001).

¹⁰W. Yim, E. Stofko, P. Zanzucchi, J. Pankove, M. Ettenberg, and S. Gilbert, *J. Appl. Phys.* **44**, 292 (1973).

¹¹J. W. Gerlach, J. Menning, and B. Rauschenbach, *Appl. Phys. Lett.* **90**, 061919 (2007).

¹²M. Kawamura, Y. Tanaka, T. Kita, O. Wada, H. Nakamura, H. Yanagi, A. Magario, and T. Noguchi, *Appl. Phys. Express* **1**, 074004 (2008).

¹³C. Zetterling, M. Oestling, K. Wongchotigul, M. Spencer, X. Tang, C. Harris, N. Nordell, and S. Wong, *J. Appl. Phys.* **82**, 2990 (1997).

¹⁴T. Uchino, N. Kurumoto, and N. Sagawa, *Phys. Rev. B* **73**, 233203 (2006).

¹⁵G. A. Slack and S. F. Bartram, *J. Appl. Phys.* **46**, 89 (1975).

¹⁶Y. Kikuchi, H. Sudo, and N. Kuzuu, *J. Appl. Phys.* **82**, 4121 (1997).